Fuzzy-Decision-Making Predictive Power Control Approach to On-Grid Photovoltaic Panel

Ali Jafer Mahdi[1], Majid Aryanezhad[2]*

[1]Electrical Engineering Department, University of Kerbala, Kerbala, Iraq, ali.j.mahdi@uokerbala.edu.iq
[2]Electrical Engineering Department, Shahid Chamran University, Ahvaz, Iran, m.aryanezhad@ieee.org

Abstract

In this paper, a voltage-current mode controller is proposed to adjust both the input current and DC voltage of a boost-inverter in order to improve the performance of the photovoltaic (PV). The proposed system is based on fuzzy-making-decision predictive voltage-current controller (FPVCC). The simulation results show that in case of using the proposed FPVCC, the input current of a PV array is in the limited value (i.e., is approximate 27% of the short-circuit current of a PV panel) compared with a classical voltage controller, an over-current is passing through PV array (i.e., is about 155% of the short-circuit current). Also, the waveform of the output voltage is sinusoidal with low total harmonic distortion (THD), i.e. 4.21%, and the power obtained from a PV array with FPVCC is approximately 6 times of power obtained without a controller.

1. Introduction

A)*Motivation*

Photovoltaic (PV) panels can be categorized into two types: off-grid and on-grid. For off-grid solar panels, the main electricity is only fed from PV panels and battery bank. These systems are suitable for remote area which is typically isolated from local grid. To maximize the power withdrawn from PV panels, maximum power point tracking (MPPT) charge controller is used by converting the variable DC voltage into maximum power point voltage. The important device in off-grid solar systems is the grid inverter which takes the DC power from both PV panels and batteries then converts it into AC power to directly supply the building. The inverters are classified into two types: grid tie inverter and normal inverter. The former one converts the solar power directly to main electricity. While, the latter one converts the DC power from PV panels and battery bank to main electricity. Moreover, the latter one is used for charging the battery bank [1-2]. For grid-connected solar power systems, the building is fed from both local grid and a PV array in order to cover the consumer's own power demand and decrease electricity bills [3]. The PV panels are connected with a grid tie inverter that directly converts DC

power into AC power (220 V, 50 Hz). For grid-connected solar systems with a storage system, a MPPT charge controller, i.e. DC-DC converter, is used for charging the bank of batteries that connects with a separate inverter. The building in these systems can be supplied during power grid failure. The drawbacks of these systems are the big losses in power electronic converters and the high cost of maintenance. Basically, there are two types of grid tie inverter topologies: central inverters and micro inverters. Central inverter is the typical choice for high power solar systems. Its efficiency is better than the other type, but it misses MPPT operation for each PV panel due to the fluctuations in atmosphere, e.g. shading and clouding. For micro inverters, each PV panel has own small size inverter, which achieves optimal power conversion for each PV panel. For these inverters, if any PV panel is shaded or is not completely pointed to the sun, the total DC power is not highly affected [4].

B)*Literature survey*

Several studies have been conducted to design and analysis of grid-connected solar power systems with or without energy storage devices. Ref. [5] designed and constructed a mini-solar power plant

connected with local grid. Each part of the solar plant is modelled and analyzed in order to estimate the behavior of the grid under various operating conditions. In [6], power electronic circuits including a buck-boost converter with a full-brig inverter was presented to supply AC power with high power factor. In [6], the waveform of the output AC voltage was improved by selecting a high switching frequency for a buck-boost converter that operates in the discontinuous-current conduction-mode (DCCM) to avoid additional input inductor current controller. It is worth noting that most of grid-connected PV inverters have been assessed by using unreal solar irradiance profile such as steps and ramps or triangle ramps. Although this test evaluation is easy to perform, it may not be representing the dynamic response of the system under actual conditions [7].

C)*Contribution*

In this paper, a grid-connected solar PV power system is designed for supplying a stable ac power without batteries. The system includes a PV array connected to grid via a boost-inverter and an LC filter. Both the input current and the output DC voltage are adjusted by controlling the duty cycles of a boost converter. The purpose of controlling the input current and DC voltage is respectively, to prevent the over-current passing through a PV array and to supply a constant ac voltage. The proposed fuzzy-decision-making predictive voltage-current controller (FPVCC) is used to optimize of the output power by controlling the current and voltage simultaneously. Simulation results present a stable AC power to grid (220 V, 50 Hz) with a high power-factor and low THD.

D)*Organization of the paper*

This paper is coordinated as follows: In Section II, the proposed PV power system is presented with a real solar irradiance profile. Section III gives the modelling and design steps of the proposed system. Section IV presents the proposed FPVCC to control of voltage-current and Section V shows the simulation and performance analysis of the proposed PV power system. Conclusions are given in Section VI.

2. Diagram of the Proposed PV Power System

Figure 1 shows the diagram of the proposed solar PV power system including a PV array, which supplies a grid via a boost-inverter. Two control signals (i.e., PWM1 for adjusting both the input current and DC voltage, and PWM2 for controlling the output AC voltage) are essential to generate a reliable output power under real fluctuated irradiances. An LC filter is connected between an

inverter and the local grid to achieve a sinusoidal AC voltage.
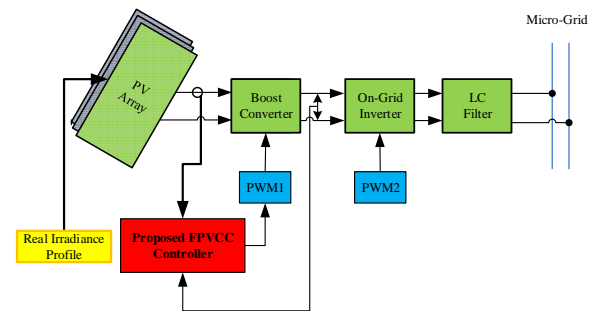
Fig. 1. Block diagram of the solar power system.

A)*Modelling and Design of the Proposed PV*

− Real Irradiance Profile:

In this paper, real solar irradiances were measured over a day in a case study in Ahvaz city as shown in Fig. 2. The curve presents how the solar irradiance changes during sunshine hours. At 1:00 pm, the sun is at the peak point, the solar irradiance is approximately 960 W/m^2. But, at 8:00 am and 6:00 pm, the solar irradiances are about 260 W/m^2 and 330 W/m^2, respectively. It is worth noting that the average solar irradiance is above 650 W/m^2, which is considered a sunny day [8].

− PV Array Simulator

PV panel is a device utilized to convert irradiance from the sun directly into DC power. Typically it made of multiple silicon solar cells joint between glass and a backing material [1]. An embedded MATLAB function is used to simulate a PV array. In literatures, a PV panel is simulated as a single diode exponential model that provides fairly accurate current-voltage characteristics, since this model does not include the effect of parallel resistance, the I-V characteristics [9]. In this paper, a PV panel is simulated as a logarithmic model using Eqs. (1)-(3) [10]. This PV model requires four input parameters, which are listed in Table 1.
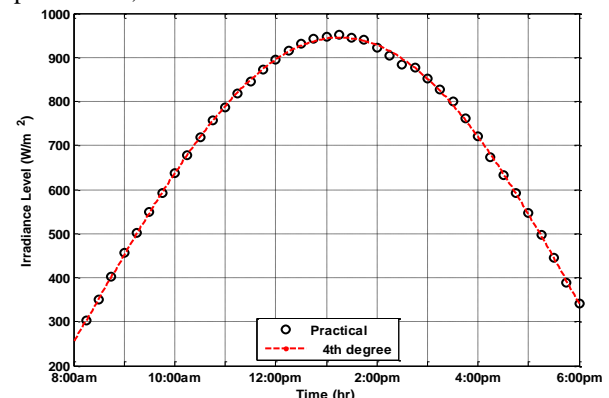
Fig. 2. Measured solar irradiances over a day in a case study in Ahvaz city

Table.1.
Parameter values of a PV panel [11]

Parameter	Value
Open circuit voltage, V_{oc}	28.4 V
Short circuit current, I_{sc}	7.92 A
Voltage at maximum power point, V_{mpp}	22.8 V
Current at maximum power point, I_{mpp}	7.11 A
Type of Array connection and number of PV panels, N_{pv}	Series, 5

$$I_{PV} = \lambda I_{sc}[1 - C_1\{\exp(\frac{V_{pv}}{C_2 V_{oc}}) - 1\}] \qquad (1)$$

$$C_1 = (1 - \frac{I_{mpp}}{I_{sc}})\exp(\frac{-V_{mpp}}{C_2 V_{oc}}) \qquad (2)$$

$$C_2 = \frac{(\frac{V_{mpp}}{V_{oc}} - 1)}{\ln(1 - \frac{I_{mpp}}{I_{sc}})} \qquad (3)$$

where λ is the per-unit solar irradiance at 1000 W/m^2.

Note that a PV panel can be also simulated as a dependent voltage-source, V_{pv}, by rearranging Eq. (1). It is clear from Eq. (4) that the PV current, I_{pv}, is firstly measured then entered to the proposed PV simulator.

$$V_{PV} = C_2 V_{oc} \ln\{\frac{1 + C_1 - (\frac{I_{pv}}{\lambda I_{sc}})}{C_1}\} \qquad (4)$$

Figure 3 shows a PV panel Simulink model based on an embedded MATLAB function and a voltage-controlled source. It is worth noting that the upper limit of PV voltage does not exceed the open circuit voltage to protect the PV panel from overvoltage damage. Figure 4 shows the proposed PV array simulator, which continues five PV panels connected in series in order to increase the DC voltage and consequently reduce the size and cost of a boost converter.

The purpose of a designing a boost-inverter is to convert DC power from PV array to a stable AC power with the following specifications: (i) constant voltage and frequency, i.e. 220 V and 50 Hz; (ii) high power factor and (iii) low total harmonics distortion (THD) for both voltage and current. In this paper, a boost converter is designed based on variable input DC voltage, (e.g., 100 V to 130 V) and using real irradiance in Fig. 2. For a boost converter, a voltage controller adjusts the duty cycle, D, to keep the load voltage constant [12] (e.g., 311 V) and load current, I_{load}, is set 2 A. In order to avoid switching losses, the switching frequency, fsw, is set to 10 kHz for the initial design. If satisfy results are obtained with this frequency, the size and cost of a boost converter are decreased [13]. The variation in

input inductor current, ΔI_{pv}, is chosen 50% less than of the average load current for all operating conditions. Furthermore, the perunit DC voltage ripple, $(\Delta V/V_{dc})$, is set less than 5%.
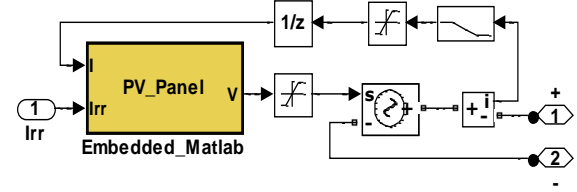
Fig. 3. Simulink model of a PV panel based on embedded MATLAB function.
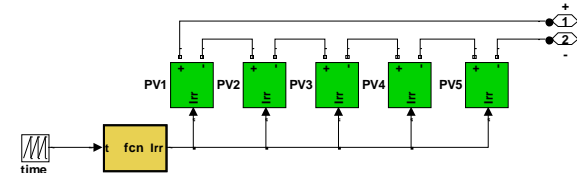
Fig. 4. The proposed PV array simulator

According to above initial design considerations, the minimum values of the boost inductor, L_{min}, and filter capacitor, C_{min}, are calculated via the following steps [12].

− Calculating D with minimum PV voltage.

$$D = 1 - \frac{V_{pv}}{V_{dc}} \qquad (5)$$

− Calculating the average value of inductor current, Ipv.

$$I_{pv} = \frac{V_{dc} I_{load}}{V_{pv}} \qquad (6)$$

− Determining the minimum inductance, L_{min}.

$$L_{min} = \frac{V_s D}{\Delta I_{pv} f_{sw}} \qquad (7)$$

− Repeating steps 1-3 for computing the maximum boost inductance, L_{max}, with maximum PV voltage.

− Finally, calculating the minimum capacitance, C_{min}, with maximum duty cycle.

$$C_{min} = \frac{D}{(\frac{V_{dc}}{I_{load}})(\frac{\Delta V}{V_{dc}})f_{sw}} \qquad (8)$$

According to above steps, the minimum values of the inductance and capacitance are approximately 2 mH and 10 μF, respectively. It is worth knowing that these values may achieve continuous mode operation. In this paper, a typical full-bridge inverter including four MOSFETs is used for DC to AC conversion. For getting a sinusoidal output voltage,

the inverter frequency (i.e., the PWM frequency of the carrier signal) is increased. Also, a sinusoidal filter (i.e., LC filter) is connected between an inverter and grid in order to obtain a smooth sine wave output voltage. As mentioned above, by increasing the inverter frequency, the cut-off frequency of an LC filter can be increased in order to decrease the size of filter inductance, L, and filter capacitance, C. Eq. (9) is used for design an LC filter at 500 Hz and the values of L and C will present in Table 2.

$$f = \frac{1}{2\pi\sqrt{LC}} \qquad (9)$$

3. The Proposed Fuzzy-Making-Decision Predictive Voltage-Current Controller

For interfacing a PV power system with grid, a boost DC-DC converter and an inverter are essential with a DC voltage controller, which has several advantages such as: (i) reducing the complexity of the PWM controller for an inverter and (ii) maintaining a high dynamic response at the AC side. In conventional PV power systems, the PV current and the output AC voltage are adjusted by two separately controllers. The former one is controlled for improving the efficiency of a PV array by adjusting the duty cycles of a boost converter, while the latter one is controlled for power quality by adjusting the input inductor current of an inverter. The key challenge in designing these controllers is generating the reference control signals under the variations of solar irradiance and load.

In this research, both the input PV current and the DC voltage are controlled by only adjusting the duty cycles of a boost DC-DC converter by FPVCC algorithm.

A)*Predictive Voltage-Current Control Scheme*

To implementation of the predictive voltage-current control (PVCC) algorithm can be divided in three main stages: current estimation, variable predictions and optimization of the cost function respect to current and voltage reference [14-15].

Predictions: The output current and voltage predictions are directly computed from the discrete model. However, the time needed to compute the DC voltage and takes a considerable portion of V_{dc}, resulting in one sampling delay. Then, variables at $(k+1)V_{dc}$ are extrapolations used as an initial condition for variables at $(k+2)V_{dc}$. Then, we must to minimization two error of cost function g_1 and g_2.

$$g_1(V_s^{k+1}) = (V_{dc}^{ref} - \hat{V}^{k+2}) \qquad (10)$$

$$g_2(V_s^{k+1}) = (\|I_{pv}^{ref}\| - \|\hat{I}_{pv}^{k+2}\|) \qquad (11)$$

For optimization of the cost function g_1 and g_2 by using of (12) the two variables prediction (V_{dc} and I_{pv}), will be pursued in one cost function G.

$$G = K_V \cdot g_1(V_s^{k+1}) + K_I \cdot g_2(V_s^{k+1}) \qquad (12)$$

Thus, the boost voltage vector that minimizes (13) is

$$V_s^{opt} = \min\ G(V_s^{k+1}) \qquad (13)$$

where, V_S^{opt} is the optimal boost voltage inverter to apply in the next sampling time. The weighting factors of (12) are two: K_v and K_I. For simplicity, the weighting factor associated with the dc voltage K_v is considered unity ($K_v = 1$) and K_I must be adjusted.

B)*Fuzzy-Making-Decision Predictive Voltage-Current Controller*

The proposed FPVCC strategy evaluates the two cost functions g_1 and g_2 in a separately fashion for each possible boost voltage converter vector saving the obtained error evaluation in two variable data structures. The operation of the FPVCC needs the specification of membership and decision functions.

$$\nabla_i(V_s^{k+1}) = \frac{g_j^{max} - g_j(V_s^{k+1})}{g_j^{max} - g_j^{min}} \qquad (14)$$

where, ∇_i is the membership function for correspondent to *i*th criterion. Therefor we choose two membership functions ∇_1 and ∇_2 for PV-current and dc-voltage respectively.

$$\nabla_1(V_s^{k+1}) = \frac{g_1^{max} - g_1(V_s^{k+1})}{g_1^{max} - g_1^{min}} \qquad (15)$$

$$\nabla_2(V_s^{k+1}) = \frac{g_2^{max} - g_2(V_s^{k+1})}{g_2^{max} - g_2^{min}} \qquad (16)$$

∇_1 and ∇_2 membership functions values to the range [0,1]. The final selection of the best voltage actuation is performed by the decision function. Then, considering that N objectives are fairly optimized a maximizing decision, minimizing decision and the *AND* operator could be stated as following;

$$\nabla_D(V_s^{k+1}) = \nabla_1(V_s^{k+1}) \cdot \nabla_2(V_s^{k+1}) \qquad (17)$$

4. Analysis of Simulation Results

In this section, the simulations are conducted in order to validate the effectiveness of the proposed controller under solar irradiances (see Fig. 2). A solar PV power system with the proposed controller is implemented in MATLAB/Simulink using power system blocks as shown in Fig. 5. Note that voltage and current sensors are applied to obtain (i) the input DC voltage and current; (ii) the AC voltage and

current and (iii) the active and reactive powers. The system parameters are given in Table 2.

A) *Performance of DC Side*

DC side includes both a PV array and a boost converter. As mentioned in Section 4, the maximum input current should be equal (or less) to the short-circuit current of a PV panel to prevent overcurrent damage. Figures (6) and (7) show the time response of transient and steady-state current of a PV array, respectively. The performance data (using a classical controller and the proposed controller), which are the peak transient PV current, Ipv_peak and PV ripple current, ΔIpv, are listed in Table 3.

Table.2.
Parameter values

Parameter	Value
Boost inductance, L, and resistance	0.6 mH, 1 mΩ
DC-link capacitance, C	100 μF
Filter inductance, L_f, and resistance	10 mH, 1 mΩ
Filter capacitance, C_f	10 μF
Load resistance, R	110 Ω
Boost switching frequency, f_{sw}	10 kHz
Inverter frequency, f_{inv}	15 kHz
Sampling period, T_s	1 μsec
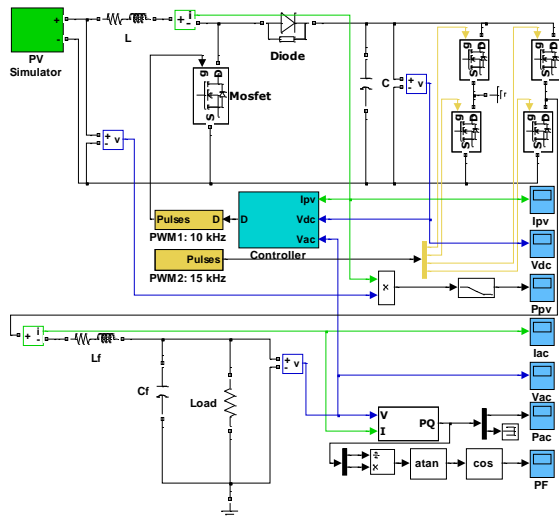
Fig. 5. Simulink model of the proposed solar-PV power system
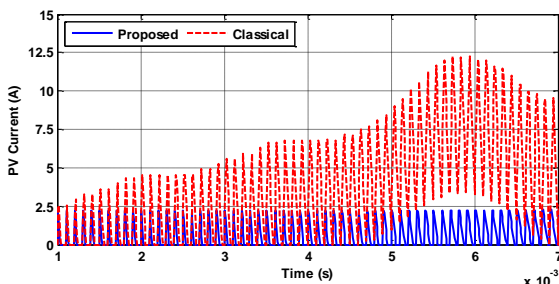
Fig. 6. PV current transient waveform
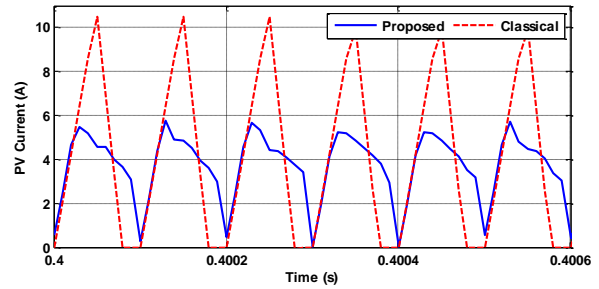
Fig. 7. PV current steady-state waveform

Table.3.
Performance of DC Side

Parameter	Classical Controller	Proposed Controller
I_{pv_peak}	12.27 A > I_{sc}	**2.19 A < I_{sc}**
$ΔI_{pv}$	10.49 A	**5.20 A**

Note that in case of using the proposed FPVCC controller, the input peak current is about 27% of Isc, while in case of using a classical controller the input current is approximately 155% of Isc. Also, in case of using the proposed controller, the ripple current is reduced to 5.2 A, while in case of using a classical controller the ripple current is 10.49 A.

B) *Performance of AC Side*

AC side includes an inverter and an LC filter. The quality assessment of a solar PV power is mainly based on: (i) keeping the output AC voltage and frequency constant; (ii) minimizing the THDs of the output voltage and current. In this research, the inverter frequency is changed in the range of 100 Hz to 15 kHz to demonstrate the quality of output voltage and current. The performance results are summarized in Table 4. It is clear that the THDs of output voltage and current at 15 kHz meet the limits proposed in IEEE standard, i.e. THD should be no higher than 5%. Figures (8) and (9) respectively illustrate the output voltage and current waveforms with their FFT analysis at 15 kHz inverter frequency.

Table.4.
Effect of inverter frequency on the quality of output V & I

Inverter Frequency	THD of Voltage	THD of Current
100 Hz	84.35%	176.25%
1 kHz	5.240%	35.28%
10 kHz	4.280%	5.450%
15 kHz	4.210%	4.650%

C) *Input and Output Power*

Figure 10 shows the input and output power (with and without the proposed controller) under real irradiances (see Fig. 2). It is seen that the output power is close to input power of a PV array and its value is increased from 100 W to 540 W due to

using the proposed control. Also, note that the power factor of a load is 0.96 lagging.
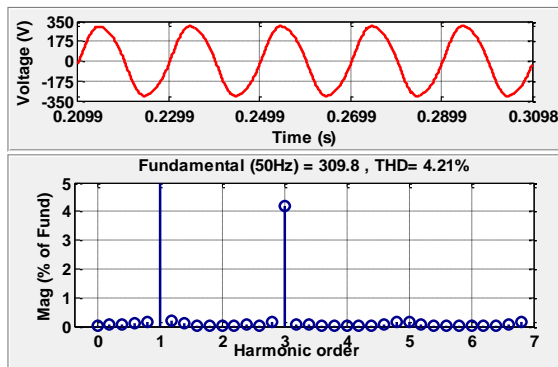
Fig. 8. FFT analysis of voltage waveform
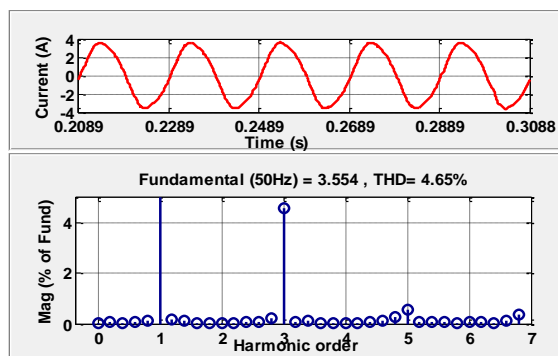
Fig. 9. FFT analysis of current waveform
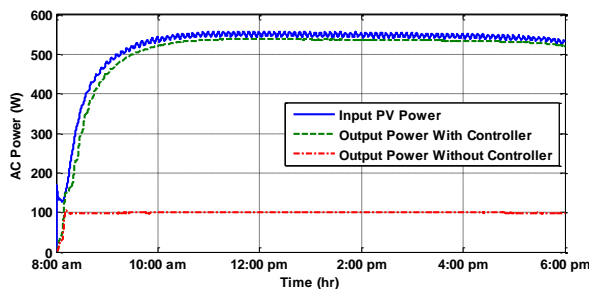
Fig. 10. Daily power waveform under real solar irradiances

5. Conclusion

This paper demonstrates the performance of a grid-connected PV power system implemented using MATLAB /Simulink under real solar irradiances of a case study. A PV array is connected with a boost inverter in order to control the input current and output voltage (as well as frequency). In this paper, the proposed voltage-current mode controller adjusts the duty cycles of boost converter under varying irradiances to keep the peak value of input current less than the short-circuit current of a PV array and to obtain a constant sinusoidal output voltage at a constant frequency. It is found that in case of using the proposed controller, the peak input current is approximate 27% of I_{sc}, compared with 155% of I_{sc} in case of using a classical controller. Also, in case of using the proposed controller, the ripple current is

reduced by 50%. Finally, with using the proposed controller, the output ac power is 5-6 times higher than without using a controller.

References

[1]   P. Gevorkian, Solar Power in Building Design: The Engineer's Complete Design Resource, McGraw-Hill Education, 2008.

[2]   G. Balazs, and P. Kiss, "Effect of Numerous PV Inverters on Power Quality Connected to the Same LV. Network in a Suburban Area," in International Conference on Renewable Energies and Power Quality, 2013.

[3]   S. Ali, N. Pearsall, and G. Putrus, "Impact of High Penetration Level of Grid-Connected Photovoltaic Systems on the UK Low Voltage Distribution Network," in International Conference on Renewable Energies and Power Quality, 2012.

[4]   G. Paul, S. Kannan, N. Johnson, and J. George, "Modeling and Analysis of PV Micro-Inverter," in International Journal of Innovative Research in Electrical, Electronics, Instrumentation and Control Engineering, vol. 2, Issue 2, 2014.

[5]   M. B. Samira, "Design and construction of a mini-solar power station connected to the electricity grid," in Elsevier BV Energy Procedia, vol. 18, 2012.

[6]   F. S. Kang, S. J. Park, S. E. Cho, and J. M. Kim, "Photovoltaic power interface circuit incorporated with a buck-boost converter and a full-bridge inverter," in Elsevier Applied Energy, vol. 82, Issue 3, 2005.

[7]   N. A. Azli, Z. Salam, A. Jusoh, M. Facta, B. C. Lim, and S. Hossain, "Effect of fill factor on the MPPT performance of a grid-connected inverter under Malaysian conditions," in IEEE 2nd International Power and Energy Conference PECon, 2008.

[8]   M. Ghazali, and A. Rahman, "The Performance of Three Different Solar Panels for Solar Electricity Applying Solar Tracking Device under the Malaysian Climate Condition," in Canadian Center of Science and Education Energy and Environment Research, vol. 2, no. 1, 2012.

[9]   F. A. Salem, "Modeling and Simulation issues on Photovoltaic systems, for Mechatronics design of solar electric applications," IPASJ International Journal of Mechanical Engineering IIJME, vol. 2, Issue 8, 2014.

[10] M. S. Benghanem, and S. N. Alamri, "Modeling of photovoltaic module and experimental determination of serial resistance," in Journal of Taibah University for Science JTUSCI, vol. 2, 2009.

[11] A.J. Mahdi, W.H. Tang, and Q.H. Wu, "Improvement of a MPPT Algorithm for PV Systems and Its Experimental Validation," in International Conference on Renewable Energies and Power Quality, 2010.

[12] D. W. Hart, Power Electronics, McGraw-Hill Education, 2011.

[13] M. Madsen, A. Knott and M. A. E. Andersen, "Low Power Very High Frequency Switch-Mode Power Supply with 50 V Input and 5 V Output," in IEEE Transactions on Power Electronics, vol. 29, no. 12, 2014.

[14] M. Aryanezhad, "Optimization of grid connected bidirectional V2G charger based on multi-objective algorithm", 8th Power Electronics, Drive Systems & Technologies Conference (PEDSTC), 2017.

[15] C. A. Rojas, J. Rodriguez, S. Kouro and F. Villarroel, "Multiobjective Fuzzy-Decision-Making Predictive Torque Control for an Induction Motor Drive,", IEEE Transactions on Power Electronics, vol. 99, 2016.